Two-color femtosecond strobe lighting of coherent acoustic phonons emitted by quantum dots

Emmanuel Péronne, Eric Charron, Serge Vincent, Sébastien Sauvage, Aristide Lemaître et al.

Related Articles

Additional information on Appl. Phys. Lett.

Two-color femtosecond strobe lighting of coherent acoustic phonons emitted by quantum dots

Emmanuel Péronne,[1,a)] Eric Charron,[1] Serge Vincent,[1] Sébastien Sauvage,[2] Aristide Lemaître,[3] Bernard Perrin,[1] and Bernard Jusserand[1]

[1]CNRS, UMR 7588, Institut des Nanosciences de Paris, F-75005, Paris, France and UPMC Univ Paris 06, UMR 7588, Institut des Nanosciences de Paris, F-75005, Paris, France
[2]CNRS, UMR8622, F-91405 Orsay, France and Univ Paris 11, Inst Elect Fondamentale, UMR8622, F-91405 Orsay, France
[3]Laboratoire de Photonique et Nanostructures, CNRS, Route de Nozay, Marcoussis, F-91460 France

The transient acoustic pulse emitted by a single InAs quantum dots layer was measured depending on the pump wavelength. By tuning the pump wavelength through the transition energies of the GaAs barrier, the wetting layer and the quantum dots themselves, the acoustic phonon emission is shown to be strongly correlated to the electronic structure of the quantum dots layer system. The contributions of the wetting layer and the quantum dots to the acoustic signal were clearly identified and quantified by comparing different regions of the same sample containing or not quantum dots. © 2013 American Institute of Physics. [http://dx.doi.org/10.1063/1.4789872]

Acoustic wavelengths as short as 5 nm can been obtained in the framework of picosecond laser ultrasonics applied to very thin metallic transducers or semiconductor multilayers.[1,2] Such acoustic pulses could be used in SONAR-like experiments on buried nanostructures with a resolution of few nanometers only. However, the laser spot diameter remains in the micron range and limits the emission wavevectors to directions perpendicular to the illuminated area. Lateral resolution down to a few hundred nanometer has been evidenced in some specific cases using clever excitation process[3] or diffraction.[4] One way to overcome this limited resolution is to use nanostructures with transverse dimensions as small as a few nanometers. Quantum dots (QDs) grown by molecular beam epitaxy (MBE) are good candidates as nano-emitters because of their small lateral size (typically 20 nm). They are embedded in a crystalline matrix with a low acoustic impedance mismatch where the propagation of very high acoustic frequency waves is possible at low temperature. Previous experiments reported that sample containing Stransky-Krastanov (SK) growth QDs layer could emit acoustic pulses.[5–7] However, it is not clear yet what is the mechanism of transduction in such systems and how the dynamics of photo-injected carrier affects the acoustic pulse. Since SK QDs stand on a wetting layer (WL) which forms a quantum well (QW) and since QWs are known to emit sound when excited by femtosecond pulses[8,9] through a deformation potential mechanism, the acoustic signal previously reported can originate mainly from the wetting layer and not from the quantum dots themselves which do provide the laterally confined emission aimed in this work. Matsuda et al. have shown that deformation potential model neglecting carrier-carrier scattering and others carrier-phonon scattering works well to explain the signal observed in QW.[9] Calculations performed on ideal spherical GaAs QD dot and including deformation potential coupling by Vagov et al.[10] show that impulsive optical excitation generates a phonon pulse propagating away from the QD. Therefore, the question of the origin of the SK QD transduction and its efficiency with respect to other nano-systems such as quantum wells remains open.

In this letter, we answer these two questions by performing picosecond laser ultrasonic experiments at 80 K on a single InAs/GaAs QD layer based on a femtosecond strobe lighting technique also known as ASOPS for asynchronous optical sampling.[12] Since the experimental set up is based on two independent femtosecond oscillators, the QDs phonon emission is triggered by pump pulses with photon energy tuned across the bandgaps of the sample, whereas the probe photon energy is kept constant. Moreover, the sample was grown such that SK growth mode has occurred on one part of the wafer only. The aim of investigating such sample with such technique is to clarify whether the sound emitted by the QD/WL layer does originate from 3D localized states and to compare the relative emission efficiency of the QD layer compared to the WL.

1.7 monolayer of InAs (critical thickness for the SK growth mode) was grown by MBE on a 2 in. GaAs[100] wafer and capped by 300 nm of GaAs. The sample rotation was interrupted during the InAs growth to provide an InAs thickness gradient along one in-plane direction. Hence, one part of the wafer contains a single In(Ga)As 2D layer, i.e., a quantum well, whereas the other part contains self-organized QDs sitting on a In(Ga)As wetting layer. The sample structure is sketched in Fig. 1. These two areas, labeled 2D and 0D, respectively, are separated by a transition area where the SK QDs density decreases progressively to zero. The sample areas were identified by photoluminescence (PL) experiment at 80 K. When scanning along the InAs gradient, the WL photoluminescence peak stands around 1.43 eV in the 2D area, shifting down to 1.40 eV and getting progressively shadowed by the QDs photoluminescence peaks arising around 1.34 eV in the transition area. The peak shifts down to 1.25 eV in the 0D area.

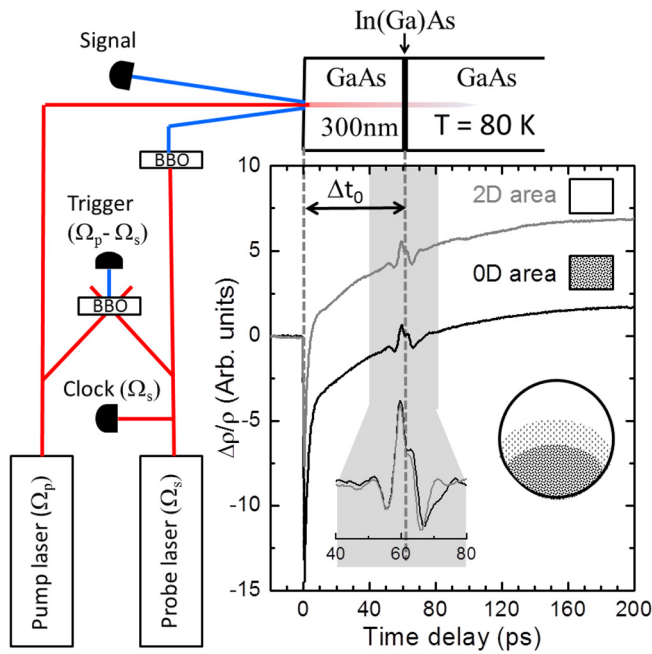a)Electronic mail: emmanuel.peronne@insp.jussieu.fr.

FIG. 1. Differential reflectivity vs time delay measured at 3.02 eV and for pump photon at 1.57 eV, either recorded in the parts with QD (0D) or without QDs (2D). The set-up is sketched on the left. The sample structure is reminded on the top and scaled to the pump-probe delay. The top view of the sample displays the areas with (0D) or without (2D) QDs and the transition area.

Carriers are photo-generated in the sample by 80-fs laser pulse originating from a Ti:Sa oscillator which operates at $\Omega_p \approx 80.000$ MHz (see Fig. 1). The pump photon energy E_p is tuned from 1.57 eV (i.e., $\lambda = 790$ nm) down to 1.29 eV (i.e., $\lambda = 960$ nm). The half width at half maximum (HWFW) of the laser spectrum is measured around 8 meV which is comparable to the WL HWHM PL peak (10 meV in the 2D area and up to 17 meV in the transition area) and smaller than the QDs PL HWHM which remains constant around 32 meV over the sample. The photo-elastic response of the sample is probed at 3.02 eV (i.e., 410 nm) by frequency doubling the output of another Ti:Sa oscillator operating at $\Omega_s \approx 79.998$ MHz. The pump-probe signal is obtained from a balanced detector and sampled by a digitizer with a clock equal to Ω_s. The acquisition is triggered every $\frac{1}{\Omega_s - \Omega_p} \approx 500 \,\mu s$ by the cross-correlation of pump and probe pulses through a BBO crystal. Consequently, changes in reflectivity $\frac{\Delta\rho}{\rho}$ are measured over 12.5 ns with a time step equal to $\frac{\Omega_p - \Omega_s}{\Omega_p \Omega_s} \approx 0.3$ ps. Due to the laser jitters, the effective time resolution increases with the numbers of scans and the pump-probe delay up to 0.5 ps for all the measurements presented in this paper.

The probe photon energy of 3.02 eV has been chosen close to the E_1 band gap of GaAs where the photo-elastic coefficient is known to be large.[13] Since the penetration depth at such a photon energy is small ($\leq$20 nm), only changes of the optical index close to the surface of the capping layer are probed. Typical signal of the relative reflectivity change $\frac{\Delta\rho}{\rho}$ at 80 K is shown in Fig. 1 depending on time and for E_p = 1.57 eV, above GaAs band gap. The signal measured in the 0D and in the 2D areas displayed the same overall behavior: a fast transient related to photo-created carriers at the sample's surface followed by a slow rising background due to

sample heating and further carriers relaxation. An extra feature appears at $\Delta t_0 = 61$ ps, the time it takes for the acoustic phonon to travel through the GaAs capping layer. This is the signature of the acoustic pulse emitted by the photo-excited In(Ga)As layer. Hence, Fig. 1 shows that an acoustic pulse is emitted by the QD/WL layer when carriers are photo-injected above the barrier band gap $E_p > E_g^{GaAs}$ as it has already been observed for InAs/InP QDs[6] at room temperature. After background subtraction (see insert Fig. 1), both signals are simultaneous and look very much alike in shape and amplitude. The main difference is occurring after Δt_0 but it is hard to conclude what part of the signal measured in the 0D case can be assigned to QDs.

By tuning the pump photon energy E_p from 1.57 eV to 1.33 eV, the signal is recorded: above the GaAs energy band gap $E_g^{GaAs} = 1.49$ eV, below the WL energy band gap $E_g^{WL} = 1.4$ eV or in between. To illustrate the effect of the pump tuning, the acoustic signal recorded above and below each band gap measured in the 0D and 2D areas is plotted in Fig. 2. When the carriers are injected at an energy just below the GaAs barrier ($E_g^{WL} < E_p < E_g^{GaAs}$), the acoustic signal is still observed either in the 0D or the 2D area with very similar shape and amplitude. Therefore, the WL alone can explain the main features of the acoustic signal observed when the pump energy $E_p > E_g^{WL}$. However, when E_p is tuned below the WL band gap ($E_p < E_g^{WL}$), the acoustic signal persists in the 0D area only: this is the first clear experimental evidence of an acoustic phonon pulse emitted by a QDs layer and which cannot be attributed to the underlying wetting layer alone. Moreover, the arrival time remains constant within 0.5 ps whatever the pump energy and the probed area. This demonstrates that diffusion, carriers capture, and relaxation have to occur faster than 0.5 ps to affect the acoustic pulse triggering. The deformation potential should be the dominant acoustic triggering mechanism since piezo-electricity can be ruled out for longitudinal wave emitted in the [100] direction which is not piezo-active. Therefore, one can expect the

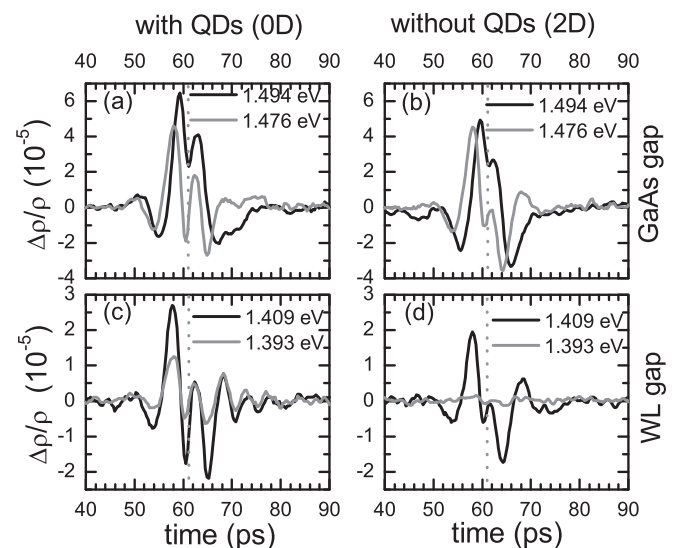

FIG. 2. Relative change of reflectivity ($\frac{\Delta\rho}{\rho}$) with pump photon energy above (1.494 eV) (a) and below (1.476 eV) E_g^{GaAs} (b), and above (1.409 eV) and below (1.393 eV) E_g^{WL} ((c) and (d)). The signal is measured in the 0D ((a) and (c)) and the 2D areas ((b) and (d)). Acoustic pulses reach the surface of the sample at Δt_0 marked by vertical dotted lines.

emission of an acoustic pulse $\eta(z, t)$ proportional to the deformation potential and to the change of carrier density created right after the photo-injection (see Ref. 14). Later on, injected carriers relax by phonon emission, therefore inducing a thermal stress which generates also an acoustic pulse by itself. Since the intraband carrier relaxation times are faster than the time resolution of the experiment when $E_p > E_g^{WL}$, both pulses should be measured simultaneously. However, they should display different E_p dependence:[14] while both are proportional to the change of electron density, the thermal contribution is also proportional to the energy differences $E_p - E_g^{i=GaAs,WL}$.

The time average $p = \langle |\frac{\Delta\rho}{\rho}|^2 \rangle_t$ is plotted in Fig. 3 depending on the photon energy E_p. It is possible to estimate from this quantity the acoustic power P_{ac} emitted by the QD layer. Indeed, when the strain pulse $\eta(t - \frac{z}{c_s})$ traveling with a velocity c_s through the cap layer is reflecting on the sample surface, the optical reflectivity (at the wavelength λ) is perturbed by a small quantity $\Delta\rho$ such as $\frac{\Delta\rho}{\rho} = R(f)\eta(f)$ in the Fourier domain where $R(f)$ is the photo-elastic response function. Since the signal only changes when E_p is crossing the band gaps, the shape of the acoustic pulse is expected to follow the same trend. Therefore, $P_{ac} \propto \int |\eta(f)|^2 df$ becomes proportional to $p \propto \int |R(f)|^2 |\eta(f)|^2 df$. When $E_p > E_g^{GaAs}$, the acoustic power is quite comparable in both areas and increases with photon energy. When $E_g^{GaAs} > E_p > E_g^{WL}$, P_{ac} remains constant with a slightly larger amplitude in the 2D region. Last, when $E_p < E_g^{WL}$, P_{ac} drops to below the experimental noise in the 2D region, whereas the 0D area still emits phonons (see expanded curves in Fig. 3(b)). The acoustic power dependence in the 0D case is remarkably similar to WL band tail Kammerer *et al.* have observed[16] by PL experiment. Data have been fitted with an error function and a square root function to reproduce, respectively, the typical 2D and 3D densities of states expected for a thin In(Ga)As QW and bulk GaAs. The quality of the fit does not require to add terms proportional to $E_p - E_g^{i=GaAs,WL,QD}$ and thus demonstrates that the thermal stress is negligible as compared to the deformation potential mechanism.

The likely transduction mechanism is the following: photons from the pump pulses are absorbed populating the conduction bands and the valence bands of bulk GaAs, InGaAs WL, confined levels in QD and mixed WL/QD states[11] depending on the pump photon energy. This sudden

carrier injection modifies the inter-atomic potential, inducing a change in the inter-atomic distances. This transient change gives rise to an acoustic strain pulse propagating away from the illuminated area. It has also been shown theoretically for ideal spherical GaAs QDs (see Ref. 10) that impulsive excitation of a two level system lead to the formation of a phonon pulse propagating away from the QD through the deformation potential. Those phonons can be viewed as phonons in excess during the polaron build up in the QD dot.

The computation of the strain pulse $\eta(t - \frac{z}{c_s})$ is required in order to get the deformation amplitude and assert the efficiency of acoustic phonon emission by QDs. A rigorous treatment of the electron and phonon properties of the QDs is out of the scope of this paper but since the probed area is much larger than the QD typical lateral size, when $E_p < E_g^{GaAs}$ the sample can be modeled as an effective quantum well with different thicknesses and In concentrations in the 0D and the 2D areas. Thus, following Ref. 9, the generated strain can be calculated by computing the sum of the squared norm of electron and hole wave functions weighted by the associated deformation potentials. The wave functions have been calculated using a 1D Schrödinger equation with square well potentials. Following Ref. 17, we used well widths of 4 nm for the QDs and 3 nm the WL and In concentration of 0.35 and 0.11, respectively. Using band parameters from Ref. 18, the computed initial acoustic pulses are shown by insets in Figure 4. Following Ref. 14, the photo-elastic response function $R(f)$ is expressed as

$$R(f) = -\frac{\frac{\partial\varepsilon_s}{\partial\eta}}{1 - \varepsilon_s}\frac{c_s}{\lambda f}\frac{f^2}{f^2 - f_B^2 - i\Gamma_B^2} \tag{1}$$

with $f_B^2 + i\Gamma_B^2 = \frac{4\varepsilon_s c_s^2}{\lambda^2}$, the dielectric constant ε_s and $\frac{\partial\varepsilon_s}{\partial\eta}$ the photo-elastic coefficient. The following parameter values are also used: $c_s = 4.765$ nm ps^{-1}, $\varepsilon_s = 20.3 + 23.2i$ and $\frac{\partial\varepsilon_s}{\partial\eta} = 480e^{i\phi}$. Some of those values have been extrapolated[15,20,21] due to the lack of data at low temperature and ϕ is left as a free parameter. In both cases, the acoustic
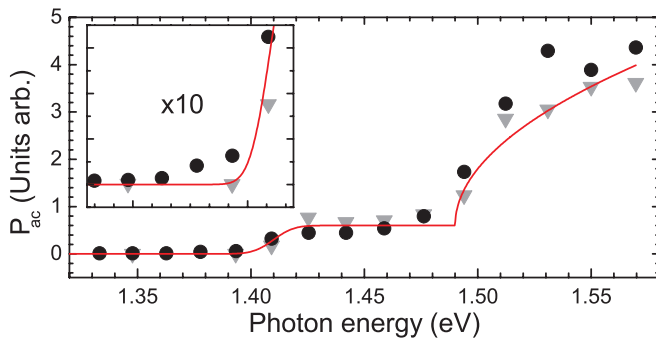

FIG. 3. Acoustic power dependence with the pump photon energy evaluated by computing the time average $\langle |\frac{\Delta\rho}{\rho}|^2 \rangle_t$ for the 0D area (circle) and the 2D area (triangle). As a guideline, the solid line display typical 2D and 3D density of state behavior when $E_p > E_g^{WL}$ and $E_p > E_g^{GaAs}$, respectively.
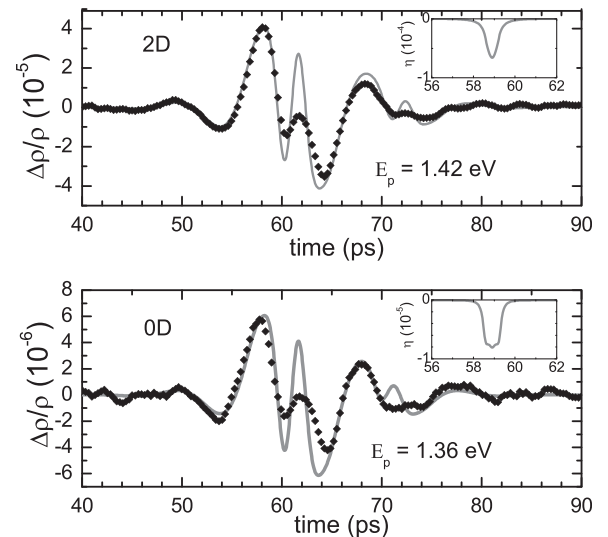

FIG. 4. Photo-elastic detection model (gray curves) applied to the corresponding strain pulses (see inserts) compared to the signal (diamond) measured: above E_g^{WL} in the 2D area and below E_g^{WL} in the 0D one.

spectrum width is broader than the photo-elastic response function which means that the overall quality of the fits are not very sensitive to the quantum well width (i.e., the well width is smaller than the optical penetration depth). Several effects have been also included for completeness: the pump-laser pulse reflection on the back of the sample which produces a 10.8 ps delayed acoustic pulse, the rms roughness measured by AFM and the apparatus jitter.

The agreement between this model and the data is qualitatively good and allows us to extract some quantitative informations. When no QDs are present, the best fit above E_g^{WL} is obtained for $\eta_0 = 6.6 \times 10^{-5}$ and $\phi = -0.07$ (see Fig. 4 (2(D))). The main discrepancy occurs around 61 ps, when the acoustic pulse is reflecting on the surface. In the QD region (see Figure 4 (0D)), the best fit at 1.36 eV (below E_g^{WL}) is obtained for $\eta_0 = 8.1 \times 10^{-6}$ (ϕ is unchanged). While the agreement is still really good before 61 ps, it is not as good as the previous one after 61 ps. Actually, this trend is observed whatever the pump energy. This may be another experimental evidence for an acoustic signature specific to the QDs layer. Indeed, this feature may reveal carrier capture and intra-dot relaxation which can last several picoseconds in QDs (instead of several hundred of femtosecond in the QW). Regarding the emission efficiency, the strain amplitudes measured above E_g^{WL} and normalized by the photo-injected carriers density are found to be comparable in both areas of the sample and also comparable to GaAs/AlGaAs QW system.[9]

By comparing results with pump energy above and below E_g^{WL} and on parts of the sample with or without QDs, the QD contribution to the acoustic signal has been isolated. The transduction efficiencies of the WL and the QDs have comparable magnitude and can be attributed to the lattice response to the sudden rearrangement of the electronic occupation after the pulse excitation. As the acoustic spectrum is mostly determined by the electronic wave functions, an improved 3D multiple band k.p model[19] would certainly yield a better description of the time dependent acoustic response around t = 61 ps where the signal is sensitive to the whole shape of the acoustic pulse. Thanks to this strong relationship between the acoustic pulse shape and the electronic wave functions, we believe that an electronic wave function tomography of nano-structures could be realized and shade new lights on carrier dynamics in such systems.

[1]N. W. Pu and J. Bokor, Phys. Rev. Lett. **91**, 076101 (2003).

[2]A. Huynh, N. D. Lanzillotti-Kimura, B. Jusserand, B. Perrin, A. Fainstein, M. F. Pascual-Winter, E. Peronne, and A. Lemaitre, Phys. Rev. Lett. **97**, 115502 (2006).

[3]K.-H. Lin, C.-T. Yu, S.-Z. Sun, H.-P. Chen, C.-C. Pan, J.-I. Chyi, S.-W. Huang, P.-C. Li, and C.-K. Sun, Appl. Phys. Lett. **89**, 043106 (2006).

[4]B. C. Daly, N. C. R. Holme, T. Buma, C. Branciard, T. B. Norris, D. M. Tennant, J. A. Taylor, J. E. Bower, and S. Pau, Appl. Phys. Lett. **84**, 5180 (2004).

[5]P. Hawker, A. J. Kent, and M. Henini, Appl. Phys. Lett. **75**, 3832 (1999).

[6]A. Devos, F. Poinsotte, J. Groenen, O. Dehaese, N. Bertru, and A. Ponchet, Phys. Rev. Lett. **98**, 207402 (2007).

[7]P. A. Mante, A. Devos, and A. Le Louarn, Phys. Rev. B **81**, 113305 (2010).

[8]J. J. Baumberg, D. A. Williams, and K. Köhler, Phys. Rev. Lett. **78**, 3358 (1997).

[9]O. Matsuda, T. Tachizaki, T. Fukui, J. J. Baumberg, and O. B. Wright, Phys. Rev. B **71**, 115330 (2005).

[10]A. Vagov, V. M. Axt, and T. Kuhn, Phys. Rev. B **66**, 165312 (2002).

[11]S. Sauvage, P. Boucaud, J. M. Gerard, and V. Thierry-Mieg, Phys. Rev. B **58**, 10562 (1998).

[12]A. Bartels, R. Cerna, C. Kistner, A. Thoma, F. Hudert, C. Janke, and T. Dekorsy, Rev. Sci. Instrum. **78**, 035107 (2007).

[13]P. Etchegoin, J. Kircher, M. Cardona, C. Grein, and E. Bustarret, Phys. Rev. B **46**, 15139 (1992).

[14]C. Thomsen, H. T. Grahn, H. J. Maris, and J. Tauc, Phys. Rev. B **34**, 4129 (1986).

[15]The sound velocity is given by temperature dependence of elastic constant found in Ref. 20 and supposing constant mass density. Dielectric constant has been obtained by interpolating measurements carried at 22K and 252 K in Ref. 21. We only know of photo-elastic coefficient measured at room temperature.[13] Thus, we have decided to use the value measured at 2.93 eV, the E1 energy gap at room temperature, as starting value for the photo-elastic coefficient around 3.025 eV the E1 gap at 80 K. Extracting a precise photo-elastic constant from experimental data is, in fact, hampered by the proximity of the E_1 gap around 3.025 eV which leads to a rapid variation of the phase.

[16]C. Kammerer, G. Cassabois, C. Voisin, C. Delalande, Ph. Roussignol, and J. M. Gérard, Phys. Rev. Lett. **87**, 207401 (2002).

[17]A. Lemaître, G. Patriarche, and F. Glas, Appl. Phys. Lett. **85**, 3717 (2004).

[18]I. Vurgaftman, J. R. Meyer, and L. R. Ram-Mohan, J. Appl. Phys. **89**, 5815 (2001).

[19]C. Kammerer, S. Sauvage, G. Fishman, P. Boucaud, G. Patriarche, and A. Lemaitre, Appl. Phys. Lett. **87**, 173113 (2005).

[20]R. I. Cottam and G. A. Saunders, J. Phys. C **6**, 2105 (1973).

[21]P. Lautenschlager, M. Garriga, S. Logothetidis, and M. Cardona, Phys. Rev. B **35**, 9174 (1987).